ACS APPLIED MATERIALS & INTERFACES

Research Article

Cite This: ACS Appl. Mater. Interfaces 2017, 9, 44900−44910

www.acsami.org

Tuning Bacterial Attachment and Detachment via the Thickness and Dispersity of a pH-Responsive Polymer Brush

Vivek Yadav,[†] Yuly Andrea Jaimes-Lizcano,[†] Narendra K. Dewangan,[†] Nayoung Park,[†] Tzu-Han Li,[§] Megan L. Robertson,*[,†,‡] and Jacinta C. Conrad*[,†]

[†]Department of Chemical and Biomolecular Engineering, [‡]Department of Chemistry, and [§]Materials Engineering Program, University of Houston, Houston, Texas 77204, United States

Supporting Information

ABSTRACT: We investigated the effect of two brush parameters, thickness and dispersity in the molecular weight distribution, on the adhesion of bacteria to pH-responsive poly(acrylic acid) (PAA) brushes synthesized using surface-initiated atom transfer radical polymerization. The attachment and detachment of *Staphylococcus epidermidis* to PAA brushes at pH 4 and pH 9, respectively, were examined with confocal microscopy. An optimal range of brush thickness, 13−18 nm, was identified for minimizing bacterial adhesion on PAA brushes at pH 4, and bacterial attachment did not depend on the brush dispersity. Increasing either the brush thickness or dispersity detached bacteria from the brushes when the pH was increased from 4 to 9. Bacterial detachment likely arose from an enhanced actuation effect in thick or high-dispersity brushes, as PAA brushes change conformation from collapsed to extended states when the pH is increased from 4 to 9. These results suggest that manipulating the molecular weight distribution provides a route to separately tune the attachment and detachment of bacteria.

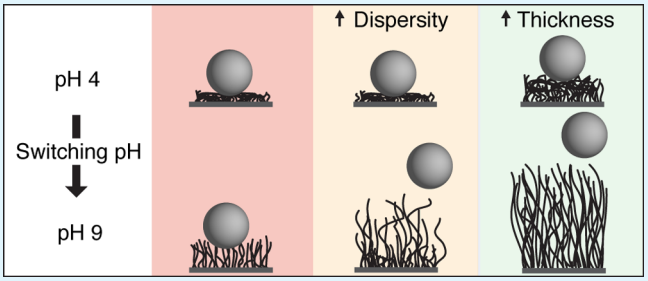

KEYWORDS: *antifouling, polymer brushes, pH-responsive polymers, bacterial attachment, bacterial detachment, Staphylococcus epidermidis*

INTRODUCTION

The formation of biofilms, surface attached colonies of microorganisms,[1] reduces the performance of water purification systems,[2] food packaging equipment,[3] and marine engineering equipment,[4] thereby posing a pressing challenge for many industrial processes. Biofilms on medical implants[5] deleteriously affect human health, causing or worsening more than 80% of hospital-acquired infections.[6] As one example, the common infectious agent *Staphylococcus epidermidis* is highly resistant to antibiotics.[7] Its virulence is often attributed to the formation of resistant biofilms after bacteria attach to medical devices.[8] Although the adverse consequences of biofilms are widely known, in other settings, they may have beneficial properties. Biofilms of select bacterial species (*Pseudomonas spp.* and *Pseudomonas putida*), for example, are used to remediate water,[9] and benign biofilm coatings on medical devices can prevent infection by pathogenic invaders.[10] In the early stages of biofilm formation, bacteria attach to surfaces reversibly and then irreversibly.[11] Hence, an important step in managing biofilm formation, whether harmful or benign, is to tailor surfaces to control the initial attachment of bacteria.[12]

In the absence of adhesins, adhesion of bacteria to a surface is governed by Lifshitz−van der Waals, hydrophobic, acid−base, and electrostatic interactions.[13] Lifshitz−van der Waals and hydrophobic interactions are typically attractive, whereas acid−base and electrostatic interactions can be either repulsive or attractive. In principle, adhesion can be tuned by coating the surface to vary its properties and hence these interactions. Polymers are a convenient choice for coatings because of their easy applicability and processability. A variety of polymer coatings have been studied to control bacterial adhesion, including zwitterionic and cationic polymers, poly(acrylamides), poly(acrylates), and poly(ethylene glycol) (PEG).[14] Their antifouling efficacy can depend, in part, on the structure of the polymer coating. Grafting polymers to a surface to form a polymer brush is often performed to create coatings, as polymer brushes favorably modulate bacteria−surface interactions to reduce adhesion. Polymer brushes reduce attractive interactions by increasing the separation between the bacteria and the surface and enhance repulsive interactions by increasing steric hindrance.[15,16] Polymer brushes can swell when solvated, depending on chemistry. Hence, the hydration of a polymer layer also can reduce adhesion by reducing attractive hydrophobic interactions. Indeed, easily hydrated polymer brushes such as PEG and zwitterionic polymers considerably reduce bacterial adhesion.[17−22]

Received: September 22, 2017
Accepted: December 7, 2017
Published: December 7, 2017

DOI: 10.1021/acsami.7b14416
ACS Appl. Mater. Interfaces 2017, 9, 44900−44910

Adhesion of organisms depends on many properties of polymer brushes, including their grafting density,[16,23] average thickness,[15,22] wettability,[24,25] and surface charge.[26,27] Expanding the range of brush properties that can be tuned opens new avenues for the design of antifouling surfaces. One characteristic property of polymer brushes, known to change their conformation and interactions[28−31] but underexplored[32] in the context of fouling, is the dispersity (breadth) in the molecular weight distribution. To our knowledge, there are no experimental studies probing the effect of brush dispersity on bacterial adhesion. Dispersity is an appealing parameter to tune in applications requiring control over adhesion because it affects the conformation of polymer brushes. Theoretical studies showed that polymer brushes exhibit extended conformations upon increasing the dispersity.[28,33,34] Moreover, simulations demonstrated that dispersity may affect adhesion of microscale particles by altering the number of contacts between particles and polymers.[29]

Despite the detailed insights provided by careful studies of adhesion on polymer brushes, static surfaces are nonetheless irrevocably fouled by bacteria. Certain aquatic organisms have developed a clever strategy to overcome this limitation: active cleaning. Mollusks and corals, among others, shed foulants through active deformation and motion,[35] and similar changes in brush conformation may promote fouling release. Stimuli-responsive polymers, as one example, change conformation and properties in response to environmental changes and represent a simple realization of the smart cleaning behavior observed in marine organisms. Hence, several stimuli, including temperature,[36−38] pH,[27,39,40] ionic strength,[41] pressure,[42] and light,[43,44] have been used to tune bacterial attachment to and detachment from responsive polymer materials. How the molecular weight distribution of the polymer affects the fouling-release properties of stimuli-responsive brushes, however, is unexplored. Both thickness and dispersity can change the conformation of a stimulus-responsive polymer brush,[45,46] suggesting that these parameters may affect the detachment of microscale particles or bacteria after stimulation. This question has not been explored experimentally, in part because of the difficulty in synthesizing polymer brushes of a wide range of dispersities and thicknesses.

Here, we investigated the effect of brush thickness and dispersity on the initial attachment and subsequent detachment of *S. epidermidis* from a model pH-responsive brush, poly(acrylic acid) (PAA). PAA brushes are neutral, collapsed, and hydrophobic at low pH and become negatively charged, swollen, and hydrophilic at high pH. We synthesized PAA brushes with controlled brush thickness and dispersity using surface-initiated atom transfer radical polymerization (SI-ATRP) and characterized the attachment and detachment of bacteria using confocal microscopy. Adhesion of bacteria on neutral, collapsed brushes at pH 4, as quantified via surface coverage (SC), varied nonmonotonically with the average brush thickness but was independent of brush dispersity. The lowest attachment occurred over a thickness range of 13−18 nm because of competing van der Waals, electrostatic, and hydrophobic interactions. When the solution pH was switched to 9, upon which the brush was charged and swollen, increasing either the dispersity or thickness promoted the detachment of bacteria from the brush surface. We suggest that an actuation effect, arising from the swelling of the polymer brushes, removes the bacteria. Increases in removal likely arise from stimulus-driven changes in brush conformation that are enhanced by greater thickness or dispersity, in turn increasing the swelling. Our results suggest that the initial attachment and detachment of microscale bacteria can be separately tuned via the molecular weight distribution of a stimulus-responsive polymer brush. Beyond potential applications for smart antifouling surface coatings, this capability may prove useful in controlled release, sensors, and separation technologies.

MATERIALS AND METHODS

Materials. All chemicals were purchased from Sigma-Aldrich and used as received, unless otherwise stated. *tert*-Butyl acrylate (*t*BA, 98%) was passed through a silica gel column (60 Å pore size), dried with calcium hydride (reagent grade, 95%), and distilled under vacuum.

Synthesis of PAA Brushes. Our initiator attachment and polymerization procedures are reported in detail in our previous publication.[46] Briefly, 1 cm × 2 cm silicon wafers (Mechanical Grade, University Wafers) or glass coverslips (VWR, 22 mm × 40 mm × 0.15 mm) were sonicated, dried, and exposed to air plasma. The substrates were exposed to (3-aminopropyl)triethoxysilane (99%) in vacuo (30 min, 50 mTorr), annealed (110 °C, 30 min), and immersed in 2 vol % anhydrous pyridine (99.8% pure) in dry dichloromethane (JT Baker, HPLC grade, 99.8%, obtained from a Pure Process Technology solvent purification system). α-Bromoisobutyryl bromide (98%) was added dropwise at 0 °C (final concentration of 0.081 M) to the solution, which was then held at 0 °C for 1 h and at room temperature for 12 h. Initiator-grafted substrates were rinsed with acetone, dried under nitrogen, and used immediately. To grow poly(*tert*-butyl acrylate) (P*t*BA) brushes from the substrates, *t*BA, *N*,*N*,*N*′,*N*′,*N*″-pentamethyldiethylenetriamine (99%, degassed prior to use), copper(I) bromide (CuBr, 99%), anhydrous *N*,*N*-dimethylformamide (99.8%), ethyl α-bromoisobutyrate (EBiB, 98%, degassed prior to use), and phenylhydrazine (97%, an additive to vary the dispersity of polymer brushes[46]) were added to a 100 mL round-bottom flask containing the initiator-grafted substrates, annealed at 50 °C for 24 h, and then quenched with excess tetrahydrofuran (THF, OmniSolv, HPLC grade, 99.9%) in air. P*t*BA-grafted substrates were rinsed with acetone, methanol (ACS reagent, 99.8%), and deionized (DI) water, and dried under nitrogen. P*t*BA brushes were converted to PAA brushes through hydrolysis via addition of trifluoroacetic acid (reagent plus, 99%) in dichloromethane for 24 h. PAA brushes were rinsed with acetone and dried under nitrogen and then used for bacteria experiments the following day. Free P*t*BA (initiated from EBiB) was purified with neutral aluminum oxide, precipitated in DI water/methanol (1:1 by volume), and dried in vacuo overnight at room temperature.

Gel Permeation Chromatography (GPC). Number-average molecular weight, M_n, and dispersity, $Đ$, were characterized with a Viscotek GPC system containing two Agilent ResiPore columns, refractive index, right-angle light scattering, and low-angle light scattering detectors, and a viscometer. The mobile phase was stabilized THF (OmniSolv, HPLC grade, >99.9%) at 30 °C, with a flow rate of 1 mL min^{-1}, injection volume of 100 μL, and polymer concentration of 2−3 mg mL^{-1}. We previously reported the dn/dc value of P*t*BA measured under these conditions.[46]

Ellipsometry. The brush dry thickness was measured at five different locations on each substrate with a J. A. Woollam M-2000 spectroscopic ellipsometer. Ellipsometry data (over the wavelength range 350−900 nm) were modeled as a polymer layer on top of SiO_2, with the refractive index of each layer described by the Cauchy dispersion relation, $n(\lambda) = A + B/\lambda^2$ (A and $B > 0$). The measured phase difference and amplitude ratio were modeled with the Fresnel equation, with the brush thickness as a fitting parameter. Although we carefully dried each brush with dry nitrogen prior to ellipsometry measurements, it is difficult to ensure that the brushes are completely dry; water contained in the brush would lead to systematic (increasing) error in the brush thickness.

Bacterial Culture. *S. epidermidis* (ATCC 12228) was used as a model bacterium. Bacteria from a frozen stock were grown on a Luria−Bertani (LB)-agar plate (5 g NaCl, 5 g yeast extract, 10 g of

DOI: 10.1021/acsami.7b14416
ACS Appl. Mater. Interfaces 2017, 9, 44900−44910

Bacto-tryptone, and 15 g agar, all from BD Chemicals) for 18 h at 37 °C (NuAire Inc.). One colony from the plate was inoculated into a sterile LB medium (5 g NaCl, 5 g yeast extract, and 10 g tryptone per 1 L medium, all from BD Chemicals) and incubated in an orbital incubator shaker (SH1000, Southwest Science) at 200 rpm and 37 °C for about 10 h. Then, a second step culture was prepared by diluting the original culture 100-fold in a sterile LB medium and incubated until the bacteria reached a stationary phase (approximately 12 h). Bacteria were separated from the growth media via centrifugation at 5000*g* in a Sorvall ST 16 Centrifuge (Thermo Fisher Scientific); the supernatant was removed and replaced with 0.9% NaCl (ionic strength 154 mM), and the pellet was resuspended and centrifuged again. The pellet was again suspended in 0.9% NaCl solution, and the optical density (OD) of the solution was adjusted to 0.25 (Laxco DSM-Micro Cell Density Meter). Finally, a 3 mL aliquot was taken from the solution with adjusted OD and centrifuged. The pelleted bacteria were then suspended in 0.5 mL of DI water at pH 4. For imaging, the bacteria were stained with 2 μM SYTO 9 nucleic acid stain (Thermo Fisher). The percentage hydrophobicity of the bacteria, assessed via the microbial adhesion to hydrocarbons[47] assay with *n*-dodecane and hexadecane, was 74 ± 4 and 57 ± 3% at pH 4 and pH 9, respectively, for *n*-dodecane and 87 ± 2 and 67 ± 1% at pH 4 and pH 9, respectively, for hexadecane.

Surface Energy and Zeta Potential of Bacteria. Using negative pressure filtration, bacterial lawns were generated on membrane filters (cellulose acetate, pore diameter 0.45 μm, Advantec). Filters bearing bacterial lawns were glued to a thin layer of just-melted dental wax (Electron Microscopy Sciences) mounted on a glass slide. Next, droplets (volume ~3 μL) of DI water, ethylene glycol (99%, Sigma), or diiodomethane (99%, Sigma) were carefully deposited onto the lawns. Using a Dataphysics OCA 15EC goniometer, the contact angles of the droplets were measured at five distinct points on the lawns. Finally, the surface energy was calculated via the method of Wu[48] using algorithms that were built into the instrument's analysis package. The results are provided in Table S1.

Zeta potentials were measured using a Nicomp 380ZLS particle sizer ζ-potential analyzer. Each suspension was diluted to an OD of 0.06 at pH 4 and pH 9 with DI water for zeta potential measurements. The results are shown in Table S2.

Microscopy, Flow-Cell Experiments, and Image Analysis. A flow-cell device was created by attaching a PAA-grafted glass coverslip to a custom-machined polycarbonate flow-cell with a silicone sealant (3M), which was allowed to cure overnight. The channels in the flow-cell, of dimensions 1.2 mm × 30 mm × 3.8 mm, were filled with DI water at pH 4, and the brushes grafted to the glass surface were equilibrated in this solution for 30 min. After equilibration, the channel was flushed with fresh DI water at pH 4. Next, 300 μL of the bacteria suspension was inoculated into the channel and incubated at room temperature (21 °C) under quiescent, no-flow conditions for 3 h (estimated error: 5 min). We measured the gravitational flux of bacteria to the surface to be 0.0006 cells min^{-1} μm^{-2} (Figure S1). The bacteria attached to the polymer brush surface were visualized using a confocal fluorescence scanner (VT-Infinity3, Visitech) mounted on a Leica DM4000 inverted microscope with a 40× oil immersion lens (HCX PL APO, numerical aperture 1.25−0.75). The fluorescence in the bacteria was excited using a laser source of wavelength λ = 488 nm. Images of area 210 μm × 160 μm (672 pixels × 512 pixels) and an exposure time of 300 ms were acquired at a frame rate of 1 fps using an ORCA 200 camera (Hamamatsu) controlled by Voxcell Scan software (Visitech).

At the start of each flow experiment, bacteria that were loosely attached to the surface after the 3 h incubation were removed by flowing DI water at pH 4 at a flow rate of Q = 45 mL h^{-1} using a Fusion 200 pump (Chemyx). This flow rate corresponded to an approximate wall shear stress of $\sigma = 3Q\mu/2Wb^2$ = 12 mN m^{-2}, where W = 3.8 mm is the measured channel width, $2b$ = 1.2 mm is the measured channel height, and μ = 0.89 mPa·s is the viscosity of water. Flow was maintained until no detachment of bacteria was observed, typically for about 20 min. Thereafter, 10 images were acquired at different positions along the channel to determine the average SC by bacteria for each brush. Subsequently, the flowing medium was switched to DI water at pH 9 while the flow rate was fixed at 45 mL h^{-1}. Flow of the pH 9 solution was maintained for 20 min. Again, 10 images were acquired at different positions. Each experiment was carried out using a PAA brush that was hydrolyzed the previous day and a fresh bacteria culture.

Images acquired from the confocal microscope were analyzed using ImageJ software (NIH) and MATLAB. In all images, bacteria appeared as bright objects on a dark background. To determine the percentage of the surface covered by bacteria, a threshold was individually applied to each image using ImageJ, and the resulting binary image was analyzed using MATLAB. The SC of the attached bacteria was calculated by counting the number of white pixels in the binarized image using a MATLAB code.

RESULTS

Brush Synthesis. P*t*BA brushes of varying thicknesses and dispersities on glass coverslips and on silicon substrates were synthesized using SI-ATRP (Scheme S1), as described in our previous publication.[46] To estimate the brush thickness on the glass coverslips, a silicon substrate was added to each reaction mixture so that the thickness could be measured with ellipsometry; explicitly, we assumed that the brush thickness on the glass coverslip equaled that on the silicon substrate. A solution initiator (EBiB) was added to every synthesis, and the molecular weight M_n of the polymer brush was assumed equal to that of the solution P*t*BA polymer (following prior studies[49,50]).

The brush thickness h scaled approximately linearly with M_n, as shown in Figure 1. From the linear scaling, the grafting density of the P*t*BA brushes was estimated as $\sigma = h\rho N_A/M_n$,[50] where ρ = 1.05 g cm^{-3} is the density of P*t*BA,[50] N_A is Avogadro's number, and M_n is the molecular weight of the solution polymer. This estimate yielded a grafting density of 0.36 chains nm^{-2} for the brushes in this study; given that the

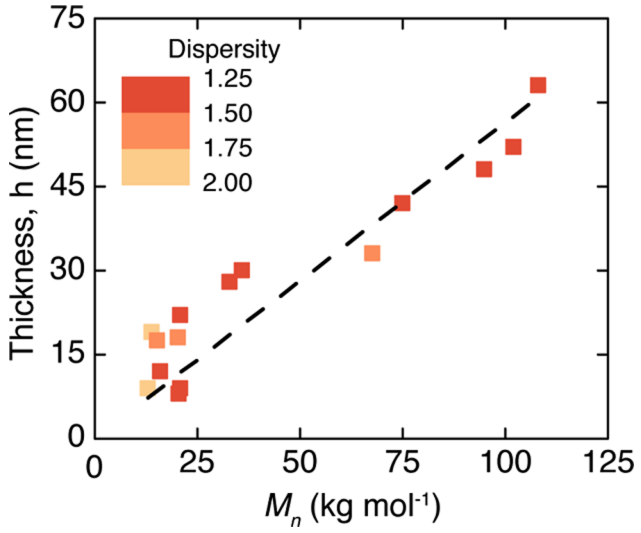

Figure 1. Dry thickness (as-synthesized) of P*t*BA brushes as a function of the molecular weight (M_n) of the P*t*BA solution polymer. Each symbol color indicates a range of brush dispersities (measured from solution P*t*BA polymers using GPC), as indicated in the legend. The error bars on each measurement represent the standard deviation over five measurements obtained from the same substrate and are smaller than the symbols. The dashed line is a linear fit through the origin (R^2 = 0.95). The grafting density for the P*t*BA brushes, calculated from the slope of the linear fit, is 0.36 chains nm^{-2}.

DOI: 10.1021/acsami.7b14416
ACS Appl. Mater. Interfaces 2017, 9, 44900−44910

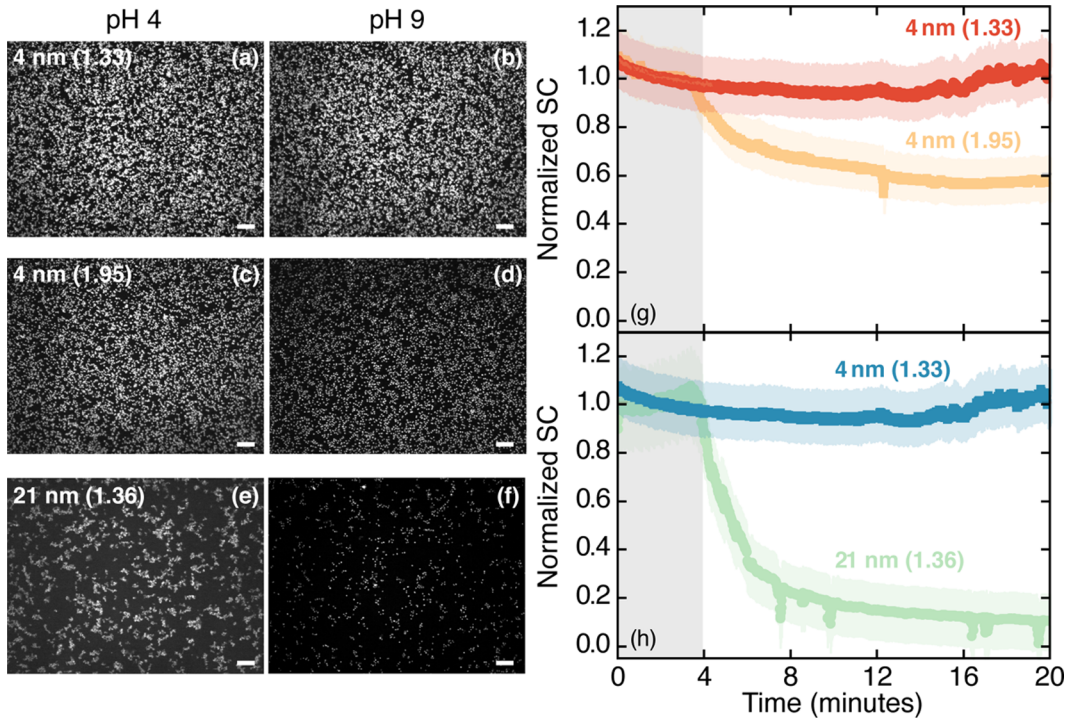

Figure 2. (a–f) Representative confocal micrographs of *S. epidermidis* bacteria deposited onto PAA brushes at pH 4 (a,c,e) and pH 9 (b,d,f). The scale bars in the images signify 30 μm. The labels indicate the PAA brush thickness (dispersity). (g,h) SC (normalized to the coverage at time t = 2 min) as a function of time after the start of the pH 9 flow for PAA brushes with varying (g) dispersity or (h) thickness. Time t = 0 indicates the start of the pH 9 flow. The error bars are estimated from the average deviation in the SC obtained by varying the threshold values of five images, over the range for which the binary image was visually similar to the actual image, and are indicated by shaded regions around each data set. The onset of detachment, ~4 min, coincides with the time required to equilibrate the flow-cell at the new pH (light gray shaded area in the plot). Increasing brush thickness and/or dispersity leads to a reduction in the SC. The sharp decrease in the coverage at some points on the curves in (g,h) is due to the adjustment of the microscope focus during the in situ experiment. Data obtained on 8–9 nm brushes of varying dispersities, showing similar trends to the 4 nm brushes in (g), are shown in Figure S4.

crossover from the mushroom to brush regime for a lower molecular weight (M_n = 8.56 kg mol^{-1}) P*t*BA brush occurred near 0.08 chains nm^{-2} [ref S0], we assumed that all brushes in this study were in the (extended) brush regime. To vary the brush dispersity ($Đ$), phenylhydrazine was added to the synthesis solution.[46] Assuming that the dispersity of the surface-attached brushes equaled that of the solution P*t*BA polymers (measured with GPC), brushes with dispersities ranging from 1.28 to 1.95 were synthesized (Table S3 and Figure S2).

The P*t*BA brushes were hydrolyzed to produce pH-responsive PAA brushes, which were characterized through Fourier transform infrared spectroscopy.[46] The thickness of PAA brushes after hydrolysis varied from 4 to 28 nm (Table S3). For all bacterial experiments, the stated thickness is that of the as-synthesized PAA (posthydrolysis) brush and the stated $Đ$ is that of the P*t*BA brush.

Interactions of *S. epidermidis* with PAA. To assess the interactions of PAA with this strain of *S. epidermidis*, we measured the hydrodynamic radius of bacteria in solutions of PAA ($M_v \approx$ 450 000 Da, Sigma-Aldrich) that were formulated at concentrations less than one-tenth of the overlap concentration, as determined from bulk rheological measurements. The hydrodynamic radius of the bacteria was nearly independent of the concentration of PAA in solution at both pH 4 and pH 9 (Figure S3). The lack of change in its size in the presence of PAA indicated that this strain of *S. epidermidis* interacted only weakly with PAA.

pH-Triggered Detachment. pH-responsive PAA brushes undergo changes in the charge and conformation as the solution pH is varied. In an acidic medium, PAA brushes are uncharged and collapsed; in a basic medium, PAA brushes are negatively charged and extended. We hypothesized that triggering the brush swelling would alter the number of adhered bacteria. We inoculated *S. epidermidis* bacteria suspended in a pH 4 solution onto PAA brushes that were equilibrated at pH 4 and thus collapsed and uncharged. The *S. epidermidis* bacteria were hydrophobic and hence readily attached to the neutral collapsed PAA brushes; loosely attached bacteria were detached by flowing the pH 4 solution at a rate of 45 mL h^{-1}. Next, the pH 9 solution was flowed through the flow-cell, causing brushes to swell and become negatively charged. We acquired confocal micrographs before, during, and after the flow of the pH 9 solution to measure changes in the coverage of the surface by bacteria as a function of the brush thickness and dispersity.

Confocal micrographs acquired before the pH 9 flow (i.e., after the pH 4 flow) and after the pH 9 flow reveal differences in the extent of bacterial attachment and detachment on surfaces of varying thicknesses and dispersities (Figure 2a–f). On a short brush of thickness 4 nm and dispersity $Đ$ = 1.33, a similar fraction of the surface was covered by bacteria before and after the pH 9 flow (Figure 2a,b). Fewer bacteria initially attached on a surface of higher dispersity ($Đ$ = 1.95) but similar thickness (4 nm); strikingly, after the pH 9 flow, there was a pronounced reduction in the SC (Figure 2c,d). Increasing

DOI: 10.1021/acsami.7b14416
ACS Appl. Mater. Interfaces 2017, 9, 44900–44910

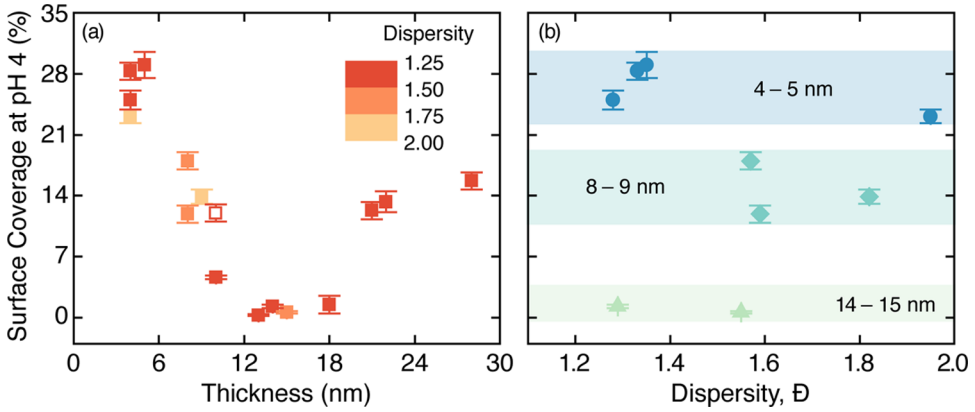

Figure 3. Percentage of the surface covered by bacteria (SC) deposited at pH 4 as a function of the (a) PAA dry brush thickness or (b) PAA brush dispersity. In (a), all brushes are included; each symbol color indicates a range of brush dispersities, as indicated in the legend. The open symbol in (a) indicates the SC for bacteria deposited from a pH 9 solution onto a PAA brush, showing that the interactions of *S. epidermidis* with PAA does not change significantly at different pH values. In (b), only brushes with similar thicknesses are compared, and the symbol shape and color indicates the thickness: 4–5 nm (●), 8–9 nm (♦), and 14–15 nm (▲). SC varies nonmonotonically with the brush thickness, attaining a minimum at an intermediate thickness, but is independent of brush dispersity for a constant brush thickness. The error bars indicate the standard deviation obtained from images taken at 10 different locations on each substrate. Horizontal bands in (b) indicate the maximum difference in the SC across the accessible range of dispersity.

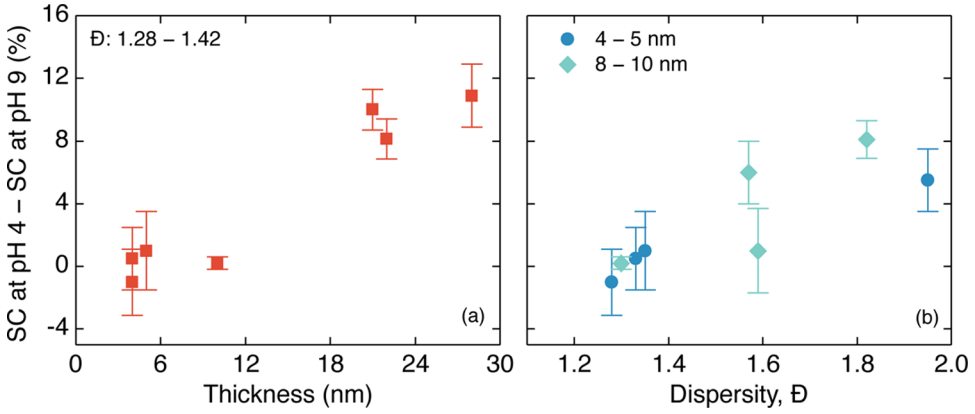

Figure 4. Reduction in the SC after switching from pH 4 to pH 9 [=SC at pH 4−SC at pH 9] as a function of the PAA brush (a) thickness or (b) dispersity. Only samples with SC > 2% at pH 4 and similar dispersity [1.28 − 1.42, in (a)] or similar brush thickness [4–5 nm (●) and 8–10 nm (♦), in (b)] are shown to separate the effects of the brush thickness and dispersity. Increasing either the brush thickness or dispersity leads to a greater release of bacteria. The error bars indicate the standard deviation obtained from images taken at 10 different locations on each substrate.

instead the thickness (to 21 nm) while holding the dispersity approximately constant (at $Đ \approx 1.3$) reduced the number of initially attached bacteria (before pH 9 flow, Figure 2e) and sharply reduced the SC after the pH 9 flow (Figure 2f). These results suggest that the brush thickness and dispersity affect the attachment and detachment of bacteria.

To gain insight into the factors controlling adhesion, we monitored the percentage of the surface covered by bacteria as a function of time, normalized to the average SC 2 min after the onset of the pH 9 flow (to account for the abrupt variation at the onset of flow at time $t = 0$). Because brushes of varying thicknesses and dispersities can exhibit pronounced differences in brush extension, charge, and conformation,[51,52] we separately examined the changes in the SC at constant $Đ$ and varying thickness and at constant thickness and varying $Đ$. The SC of bacteria on a short 4 nm PAA brush with $Đ = 1.33$ was nearly constant over the duration of the experiment. On a brush with a similar thickness but larger dispersity of $Đ = 1.95$, however, the SC began to decrease 4 min after the start of the pH 9 flow (Figure 2g), indicating that bacteria were detached from the surface. The timescale at the onset of detachment, ∼4 min, reflected the time required for the flow-cell to equilibrate at pH 9[a] and was much longer than the characteristic response time of the brush (<10 s, measured by monitoring the change in the contact angle over time for a brush equilibrated at pH 4 and exposed to a water drop of pH 10). The bacteria also detached from a longer brush of thickness 21 nm but low dispersity $Đ = 1.36$ (Figure 2h), and the onset of detachment occurred at a similar time after the pH 9 flow; the latter result confirmed that the detachment time was set by the time needed to equilibrate the solution inside the flow chamber.

Brush Thickness Controls Attachment. To probe the effects of brush thickness and $Đ$ on bacterial attachment, the average percent of the surface covered by bacteria was calculated across confocal images acquired at 10 different locations after the flow of the pH 4 solution, for which PAA brushes are collapsed and uncharged. As the brush thickness was increased from 4 to 12 nm, the SC decreased until reaching a local minimum (Figure 3a). Few bacteria were attached on brushes of thickness 13−18 nm (Figure S5). The SC increased sharply as the thickness was increased from 18 to 21 nm and then increased very slowly for the greatest thicknesses accessed

DOI: 10.1021/acsami.7b14416
ACS Appl. Mater. Interfaces 2017, 9, 44900−44910

here. To additionally confirm that the interactions of *S. epidermidis* bacteria with PAA did not significantly change with pH, we also deposited bacteria from a solution of pH 9 (open symbol in Figure 3a) onto a swollen PAA brush equilibrated at pH 9; the SC in this experiment was indistinguishable from that on brushes of comparable thickness equilibrated at pH 4. The bacteria covered a similar percentage of surfaces functionalized by brushes of comparable thickness but varying dispersities (Figure 3b), suggesting that the thickness but not dispersity predominantly controls bacterial attachment.

To test this idea, we examined the percentage of the surface covered by bacteria as a function of the brush dispersity for brushes of comparable thickness. The bacteria covered a similar (high) fraction of the surfaces of brushes of thickness 4−5 nm, even as the dispersity was varied from 1.28 to 1.95 (Figure 3b). Likewise, the SCs on brushes of thickness 8−9 nm and on thickness 14−15 nm were nearly constant, independent of dispersity. Moreover, the SC decreased as the brush thickness was increased from 4−5 to 8−9 nm and then to 14−15 nm, consistent with the data presented in Figure 3a. Together, these results indicate that $Đ$ does not affect the adhesion of bacteria; instead, adhesion is controlled by the brush thickness.

Brush Thickness and Dispersity Affect Detachment. To probe the effects of the brush thickness and $Đ$ on detachment of bacteria, we examined the change in the percentage of the surface covered before and after switching to pH 9 (i.e., before and after swelling the PAA brushes). Because it was difficult to assess meaningful changes in the fraction of surfaces with initial coverages of <2% (comparable to the magnitude of the error in the SC measurement), we compared only those samples with relatively high initial SCs at pH 4. For a series of brushes of similar dispersities ($1.28 < Đ < 1.42$), the reduction in the SC upon switching to pH 9 increased monotonically with the brush thickness (Figure 4a) (as very few bacteria attached to brushes of thickness 13−18 nm, these samples were not included in Figure 4a). We therefore conclude that thicker brushes more effectively removed bacteria when dispersity was held approximately constant. Similarly, for two series of brushes of approximately constant thickness (4−5 nm and 8−10 nm), the reduction in the SC upon switching to pH 9 increased monotonically with brush dispersity (Figure 4b). Brushes of thickness 8−10 nm were slightly more effective than those of thickness 4−5 nm in reducing the SC after pH switching because of their greater thickness. Slightly higher reductions in the SC were achieved over the studied range of brush thicknesses relative to that observed for the studied range of dispersities; a 12% reduction in the SC was observed for the longest brush in the constant-dispersity series, whereas 7−8% reduction was observed for the brushes of highest dispersity in the constant-thickness series. A dispersity of $Đ = 1.95$ is close to the maximum of 2 anticipated for unimodal size distributions formed through radical polymerization techniques. Nonetheless, these results demonstrate that increasing either the thickness or dispersity of responsive brushes promote removal of bacteria from the surface after pH switching.

DISCUSSION

Polyelectrolyte brushes such as PAA change their surface charge and conformation with the solution pH: PAA brushes are uncharged and collapsed at low pH and negatively charged and extended at high pH. Additionally, PAA brushes are hydrophobic at lower pH because of greater extent of intramolecular hydrogen bonding and are hydrophilic at higher pH because of greater extent of intermolecular hydrogen bonding.[53,54] Various analytical measurements have confirmed the changes in the wettability and thickness of PAA brushes with solution pH.[50,53−56] In our earlier study, for example, PAA brushes exhibited lower thickness and higher contact angle at low pH and higher thickness and lower contact angle at higher pH; these results coincide with expectations based on a pH-dependent conformational change.[46] Here, we tested the adhesion of bacteria on PAA brushes equilibrated at pH 4 and at pH 9 as models for tunable substrates with the ability to change the brush charge and conformation. By synthesizing brushes of varying thicknesses and dispersities, we sought to identify the effects of these brush properties on bacterial attachment and detachment. Our results, summarized in Figures 2−4, indicate that the brush thickness and dispersity differently control the attachment and detachment of bacteria from the brush surface.

Mechanism of Bacterial Release from PAA Surfaces. The results presented in Figure 2 indicate that bacteria are detached from PAA brushes of high dispersity and/or thickness when the solution pH is changed from 4 to 9; the detachment mechanism must overcome the gravitational force of bacteria on the brushes, estimated (via measurements of the sedimentation rate of bacteria, Figure S1) to be on the order 0.1 fN or lower. To understand the mechanisms driving the detachment, we first considered how changing the pH affected electrostatic interactions between the bacteria and the brushes. The isoelectric point of *S. epidermidis* bacteria is between 2.0 and 2.3,[57] and the surface charge of the bacteria did not change sign as the pH was increased in our experiments (Table S2). As the surface changed from neutral (at pH 4) to charged (at pH 9), one possibility is that the negatively charged *S. epidermidis* bacteria were repelled from the newly negatively charged PAA surface.[58,59] In this picture, brush parameters that increase the net charge upon switching the pH should enhance detachment. In support of this idea, switching copolymer brushes with a pH-responsive poly(2-carboxy ethyl acrylate) block from low pH to high pH removed *S. epidermidis* bacteria from a 24 nm copolymer brush.[27] In our system, however, very few bacteria were detached from a brush with thickness 4 nm and dispersity 1.33 compared to brushes of higher thickness and/or dispersity, although all brushes switched from neutral to charged upon increasing the pH.[46] Because the electrostatic repulsions depend on the net charge, the repulsion should increase as the molecular weight (and therefore the brush thickness) is increased; because detachment varied with dispersity at a constant thickness, it is unlikely that the change in the surface charge alone drives bacterial removal.

Instead, we suggest that detachment of bacteria from brushes with higher thickness and/or dispersity is due to an actuation effect that, in turn, arises from pH-induced conformation changes. In our earlier study, the dry thickness of a PAA brush with an as-synthesized thickness of 30 nm increased ∼40% more than that of a 6 nm (as-synthesized) brush with a similar dispersity, when pH was changed from 4 to 9. At a constant grafting density, brushes of higher as-synthesized thickness have a higher number-average molecular weight, M_n (Figure 1). Per theories for a weak polyelectrolyte brush,[45,60] we anticipate that the wet thickness of a PAA brush increases with both M_n and dry thickness. Hence, we suggest that increasing the dry brush thickness increases the extent of swelling upon switching pH from 4 to 9 and thereby increases the removal of adherent bacteria (consistent with the images in Figure 2e,f). Likewise,

DOI: 10.1021/acsami.7b14416
ACS Appl. Mater. Interfaces 2017, 9, 44900−44910

two theoretical studies suggested that increasing the dispersity of polymer brushes may promote conformations that, in turn, magnify the brush thickness: (a) neutral polymer brushes of high dispersity adopt a crown-and-stem morphology, in which the longer chains are greatly extended[33] (recently shown experimentally[31]) and (b) polymer brushes of higher dispersity exhibit extended density profiles.[28,34] We posit that electrostatic and steric repulsions arising at pH 9, when the PAA brushes are fully charged, will enhance the extension of the longer chains. Hence, we suggest that brushes of higher dispersity will extend more upon switching from pH 4 to pH 9 and thereby increase the removal of bacteria from the surface (consistent with the images in Figure 2c,d).

Our suggested physical picture for the mechanism of bacterial release is shown in Figure 5. When the brush thickness is held constant, increasing the brush dispersity $Đ$ increases the number of longer chains, which extend more than short chains when the pH is increased from 4 to 9; this extension enhances the removal of bacteria from the PAA surface. When the brush dispersity is held constant, increasing the brush thickness magnifies the extent of swelling when the pH is increased from 4 to 9, enhancing the removal of bacteria from the PAA surface. Because both thickness and dispersity are expected to monotonically increase the extent of brush swelling upon pH change, this picture also explains the results reported for detachment in Figure 4.

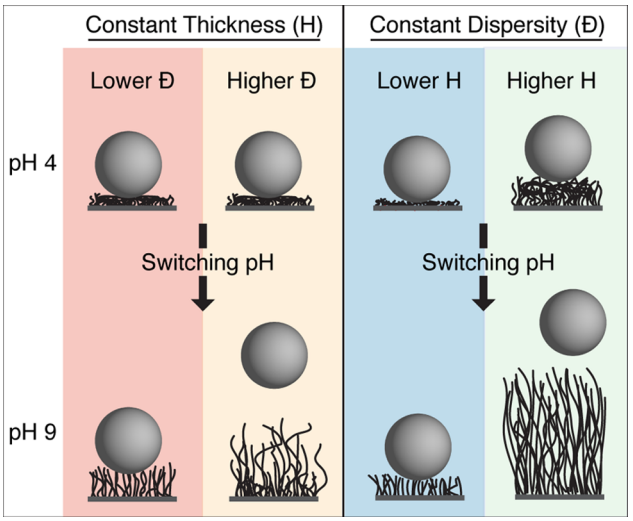

Figure 5. Illustration of the removal of *S. epidermidis* bacteria as the solution pH is rapidly switched from 4 to 9. Brushes of greater dispersity (left) or thickness (right) swell more upon increasing pH. These conformational changes reduce the bacteria−substrate interactions that drive adhesion and thereby promote the release of adherent bacteria.

Mechanism of Bacterial Attachment to Neutral PAA Brushes. The results presented in Figure 3 indicate that attachment of bacteria on the collapsed, neutral brushes at pH 4 varied nonmonotonically as the brush thickness was increased, first decreasing to a local minimum between 13 and 18 nm and subsequently increasing. Our results for short brushes are comparable to those obtained in earlier studies on antifouling polymer brushes. Attachment of *S. epidermidis* bacteria on poly(ethylene oxide) brushes, for example, decreased as the brush thickness was increased from 2 to 7 nm.[15] Similarly, attachment of *S. epidermidis* decreased as the thickness of poly(2-hydroxyethyl methacrylate) (PHEMA) brushes grafted at low density was increased from 2 to 5 nm; adhesion of bacteria on brushes grafted at higher densities, however, did not vary with the brush thickness, most likely because of negligible bacterial adhesion on PHEMA brushes.[61] Over the full range of thicknesses, the nonmonotonic dependence of attachment reported in Figure 3 is akin to that observed for a marine bacterium, *Cobetia marina*, on 10−60 nm thick random copolymer brushes of PHEMA and poly(ethylene glycol monomethacrylate) [poly(HEMA-*co*-$PEG_{10}MA$), in which $PEG_{10}MA$ had an average side-chain length of 10 ethylene glycol units]. Bacteria adhered least to poly(HEMA-*co*-$PEG_{10}MA$) brushes of thickness 20−40 nm, and attachment increased as the brush thickness was increased or decreased outside this range.[22] These results evoke the nonmonotonic dependence on the brush thickness reported for protein adsorption.[62] A variety of polyacrylamide and polyacrylate brushes bearing different functional groups exhibited ultralow fouling by proteins from blood plasma and serum at intermediate thicknesses, with two examples being poly(carboxybetaine acrylamide) [poly(CBAA)] brushes of thickness 15−25 nm and poly(*N*-acryloylaminoethoxyethanol) brushes of thickness 10−40 nm.[63−65] Poly(sulfobetaine methacrylate) and poly(serine methacrylate) brushes also exhibited local minima in protein adsorption as a function of the brush thickness, with lowest adsorption at thicknesses of 62 and 37 nm, respectively.[66,67] Insights into the properties controlling protein adhesion are suggested by the anomalous behavior of poly(hydroxypropyl methacrylate) brushes, whose high protein adsorption was attributed to its relatively high hydrophobicity.[64] Likewise, the decrease in protein adsorption between 25 and 37 °C on poly(CBAA) brushes, which become increasingly hydrophilic with increasing temperature, underlines the role of hydrophobicity on protein adsorption.[63]

In our experiments, bacteria adhered least on PAA brushes of thickness 13−18 nm, comparable to the ranges that minimized protein adsorption across acrylate and acrylamide chemistries.[62] This nonmonotonic dependence of bacterial adsorption on the brush thickness must arise from physicochemical interactions between the substrate, brush, and bacteria. One widely used model for the interaction potential between particles and a brush-coated substrate contains three interactions: (i) short-range particle−substrate interactions (e.g., ion pairing, hydrogen bonding, and hydrophobic interactions); (ii) long-range Lifshitz−van der Waals attractions between the particles and substrate; and (iii) osmotic repulsions between the particles and brushes.[68] This model assumes that particles have no affinity for the polymer brushes. The resultant interaction potential exhibits two minima, a primary minimum very near the substrate and a secondary minimum near the outer surface of the brush.[23] Particles can only adsorb in the primary minimum when they are able to reach the surface. Because our brushes are grafted at high density (0.36 chains nm^{-2}, Figure 1) and the bacteria are much larger than the average spacing between chains (~1.9 nm), we expect that bacteria mostly adsorb in the secondary minimum. The depth of the secondary minimum is governed by the competition between van der Waals attraction and steric repulsion.[68] Increasing the brush thickness reduces the depth of the secondary minimum because the strength of the van der Waals attraction decreases as the particle and the substrate are increasingly separated. Further, increasing the brush thickness also increases the steric repulsion energy[16] and the electrostatic repulsions between the brush and

DOI: 10.1021/acsami.7b14416
ACS Appl. Mater. Interfaces 2017, 9, 44900−44910

bacteria. The decrease in van der Waals attractions and the increase in electrostatic and elastic repulsions reduce adsorption of particles as the brush thickness is increased. Hence, the initial decrease in bacterial attachment with increasing thickness, reported in Figure 3a, is consistent with the model of ref 68.

This model, however, cannot explain the increase in bacterial attachment at high brush thicknesses—likely because it neglects the hydrophobic interactions between the brushes and bacteria. The enhanced adsorption of proteins on longer brushes was attributed to stronger intra- and intermolecular interactions between long polymer chains, leading to chain entanglements.[64] Stronger interactions between polymers weaken the interactions between polymers and water, reducing surface hydration; consequently, the surface becomes more hydrophobic and more proteins adsorb.[62] In our experiments, we also observed nonmonotonic dependence of bacterial attachment on thick collapsed brushes at pH 4; following refs 22 and 62, we attribute this increase to greater interactions between longer chains of thick PAA brushes. A similar argument is given in ref 22 for the attachment of bacteria to swollen and hydrated poly(HEMA-*co*-PEG_{10}MA) copolymer brushes, where attachment inversely tracked brush hydration. There, the minimum in attachment coincided with the maximum in hydration at intermediate brush thicknesses (20−40 nm), as determined using a quartz crystal microbalance experiment. Hydration decreases at lower thicknesses because the osmotic penalty to remove water from the brush is lowered;[22,62,69] hydration also decreases at higher thicknesses because of entanglements.[22]

In contrast to the striking dependence of bacterial attachment on the brush thickness, the data in Figure 3 indicate that brush dispersity does not affect the attachment of bacteria onto collapsed brushes at pH 4. This result suggests that the depth of the secondary minimum controlling the bacterial attachment is independent of brush dispersity. Thus, bacteria attached to collapsed brushes of similar average thickness but varying dispersity experience similar van der Waals attractions and steric repulsions; both are controlled by the average brush thickness, independent of dispersity. This result contrasts with a theoretical study of a neutral polymer brush, which for large particles found that increasing the dispersity in the brush molecular weight reduced the depth of the secondary minimum and shifted its position slightly further from the substrate; both effects were expected to reduce fouling by large particles.[70] The grafting density in our study (0.36 chains nm^{-2}), however, was higher than that considered in ref 70 (0.05 chains nm^{-2}); hence, it is possible that the increased steric repulsion, arising from the higher grafting density, overwhelmed a smaller difference in attraction of particles to low- and high-dispersity brushes.

The lack of dependence of attachment on dispersity remains surprising because highly disperse brushes nonetheless contain long chains, which are expected to undergo enhanced swelling upon pH change. To estimate the distribution of long chains (and thus, indirectly, the likelihood of their interactions), we calculated the molar percentage of chains of molecular weight M greater than 75.1 kg mol^{-1} (corresponding to the threshold thickness of 18 nm identified in Figure 3a) for the brushes of greatest dispersity at a given thickness in Figure 3b, using the molecular weight distribution characterized with GPC. The 4 nm brush with $Đ$ = 1.95 contained no chains with M > 75.1 kg mol^{-1}, the 9 nm brush with $Đ$ = 1.82 contained 2.3 mol % of long chains (corresponding to an areal density of 0.008 chains nm^{-2} with M > 75.1 kg mol^{-1}), and the 15 nm brush with $Đ$ = 1.55 contained 39 mol % of long chains (areal density of 0.14 chains nm^{-2} with M > 75.1 kg mol^{-1}).[b] Attachment of bacteria on these brush surfaces was indistinguishable from that on brushes of similar thickness but lower dispersity. This result suggests that the distribution, and not simply the presence, of longer chains is essential for reducing the polymer−water interactions. Likely, longer chains separated by many shorter chains cannot form the chain entanglements required to enhance polymer−polymer interactions. We therefore posit that the large separation between the long chains in highly disperse brushes prevents the polymer−polymer interactions that increase the surface hydrophobicity in brushes of large thickness. The long chains in highly disperse brushes, though, can still extend upon switching to pH 9 to promote detachment by bacteria.

Comparison to Antifouling Studies Varying Brush Grafting Density. The calculation of an effective concentration of long chains in highly disperse brushes prompts comparisons to the many studies probing the effect of brush grafting density on antifouling efficacy. As the grafting density is increased, polymer brushes undergo a structural transition from the mushroom regime (in which brushes are nearly hemispherical) to the brush regime (in which the brushes are fully extended).[71] Further, the brush thickness increases concomitant with the grafting density because of greater steric repulsion.[60,72] Together, these effects suggest that brushes grafted at higher densities should exhibit a better fouling resistance. Indeed, many studies report decreases in cell and protein adsorption upon increasing the grafting density of polymer brushes.[16,23,61,72,73] Moreover, the model of ref 68 predicts lower particle adhesion as the grafting density is increased because of the increased steric repulsion and reduced van der Waals attractions experienced by an adhering particle.[68] Although our study employed brushes in the "extended brush" regime at a fixed (total) grafting density, the lack of dependence of bacterial attachment on brush dispersity indirectly supports the idea that low areal densities (here, of the long chains that effectively repel bacterial attachment) are less effective at preventing adhesion of bacteria.

CONCLUSIONS

We show that tuning the molecular weight distribution of pH-responsive polyelectrolyte brushes yields orthogonal control over the attachment and detachment of adherent *S. epidermidis* bacteria. By synthesizing PAA brushes with varying dry thicknesses (4−28 nm) and dispersities (1.28−1.95), we quantified the effects of brush thickness and dispersity on bacterial attachment and stimulated detachment of *S. epidermidis*. Bacteria were detached from the brush surface when the solution pH was switched from pH 4 (at which PAA is uncharged and hydrophobic) to pH 9 (at which PAA is charged and hydrophilic). Brushes with very low dispersity and thickness showed negligible detachment; increasing the brush thickness and/or brush dispersity promoted bacterial detachment. By contrast, bacterial adhesion at pH 4 was independent of dispersity but varied nonmonotonically with the brush thickness.

To explain the greater detachment efficiency of PAA brushes with higher thickness and/or dispersity, we propose that conformational changes in the brush upon switching from pH 4 to 9 generated an actuation effect. Brushes of higher dry thickness and/or dispersity swelled more (due to changes in polymer chain conformation) in response to a change in pH

DOI: 10.1021/acsami.7b14416
ACS Appl. Mater. Interfaces 2017, 9, 44900−44910

from 4 to 9, releasing adhered bacteria. To explain the nonmonotonic dependence of bacterial adhesion on the dry brush thickness, we suggest that the combination of Lifshitz−van der Waals attractions, steric repulsions, and hydrophobic interactions (with the brush surface) generate a local minimum in the interaction potential of bacteria with the substrate. Bacteria attached to collapsed brushes of similar average thickness but varying dispersity experience similar van der Waals attractions and steric repulsions. Although longer polymer chains increased both polymer−polymer interactions and hydrophobic bacteria−brush interactions, the areal density of long chains remains low even at high dispersities. Hence, bacterial attachment is independent of brush dispersity. We note that PAA is not especially antifouling,[74] suggesting that the removal arises from the stimulus-induced change in conformation, and the synthetic method can be extended to the vast array of antifouling polymers that can be synthesized via ATRP.[62,65]

Our findings suggest several routes to improve the efficacy of smart coatings. First, selecting the optimum brush thickness may considerably reduce bacterial fouling. In our system, the optimal thickness is set by the competition between different physicochemical interactions. Whether this optimal thickness is constant across a range of fouling organisms, including different species of bacteria as well as macrofoulers, is not a priori clear. Reference 22 suggests that this is indeed the case for swollen (charged, hydrophilic) brushes, in which organism/brush interactions are controlled by hydration of the polymer; additional studies across a broad range of polymer chemistries with varying degrees of hydrophobicity are needed to confirm this idea. Second, employing higher brush thickness and dispersity may significantly improve the ability of smart polymers to remove foulants by magnifying changes in polymer conformation in response to a stimulus. Tailoring the distribution of polymer molecular weight is largely unexplored in the context of smart antifouling surfaces, but may provide a new route by which to enhance their antifouling properties. More generally, polymer brushes of broad dispersity may have use in other applications that demand controllably tunable adsorption and desorption of particles, including sensing, separations, and controlled release.

■ ASSOCIATED CONTENT

Supporting Information

The Supporting Information is available free of charge on the ACS Publications website at DOI: 10.1021/acsami.7b14416.

Water contact angle and surface energy of *S. epidermidis* lawns; zeta potential for *S. epidermidis* at pH 4 and pH 9; number of *S. epidermidis* cells deposited on a glass substrate as a function of time; reaction scheme of synthesis of PAA; GPC data obtained from P*t*BA polymerized in solution and resulting M_n and $Đ$ of all polymers; interaction of *S. epidermidis* with solution PAA; variation in the normalized SC as a function of time of pH 9 flow for 8−9 nm PAA brushes with varying dispersities; micrographs of PAA surfaces exhibiting very low bacterial adhesion at pH 4; calculation of free energy of electrostatic interactions between PAA brushes and bacteria; and calculation of the gravitational force of a sedimenting bacterium on brushes (PDF)

■ AUTHOR INFORMATION

Corresponding Authors

*E-mail: mlrobertson@uh.edu (M.L.R.).
*E-mail: jcconrad@uh.edu (J.C.C.).

ORCID

Megan L. Robertson: 0000-0002-2903-3733
Jacinta C. Conrad: 0000-0001-6084-4772

Notes

The authors declare no competing financial interest.

■ ACKNOWLEDGMENTS

We thank Vincent Donnelly for use of the ellipsometer, Gila Stein for use of the goniometer, and Navin Varadarajan for use of the plasma cleaner. We thank Wenyue Ding for assistance with the brush synthesis. Finally, we thank Ramanan Krishnamoorti and Richard Willson for helpful discussions. M.L.R. gratefully acknowledges support from the National Science Foundation under grant no. CBET-1437831. J.C.C. acknowledges funding from the National Science Foundation (DMR-1151133) and the Welch Foundation (E-1869).

■ ADDITIONAL NOTES

[a]The total flow cell equilibration time was calculated to be 4.07 min, which includes the time for the solution to travel through the complete tubing and flow cell volume (2.60 min) as well as the time for the flow cell to be completely mixed, modeling it as a continuously stirred reactor (1.47 min).

[b]We estimated the surface density at which the separation between long brushes is comparable to their radius of gyration in solution. This concentration, which signals the transition from the mushroom to brush regime, is estimated to be 0.003 chains nm^{-2} for a PAA brush of M_w = 75.1 kg mol^{-1} [by scaling the previously reported crossover density of 0.08 chains nm^{-2} for a lower molecular weight brush of 8.45 kg mol^{-1} [ref 50]). Hence, even the (relatively sparse) long brushes are likely extended.

■ REFERENCES

(1) Kolter, R. Surfacing views of biofilm biology. *Trends Microbiol.* **2005**, *13*, 1−2.
(2) Asuri, P.; Karajanagi, S. S.; Kane, R. S.; Dordick, J. S. Polymer−nanotube−enzyme composites as active antifouling films. *Small* **2007**, *3*, 50−53.
(3) Conte, A.; Buonocore, G. G.; Bevilacqua, A.; Sinigaglia, M.; Del Nobile, M. A. Immobilization of lysozyme on polyvinylalcohol films for active packaging applications. *J. Food Prot.* **2006**, *69*, 866−870.
(4) Chambers, L. D.; Stokes, K. R.; Walsh, F. C.; Wood, R. J. K. Modern approaches to marine antifouling coatings. *Surf. Coat. Technol.* **2006**, *201*, 3642−3652.
(5) Donlan, R. M. Biofilm formation: A clinically relevant microbiological process. *Clin. Infect. Dis.* **2001**, *33*, 1387−1392.
(6) Romero, R.; Schaudinn, C.; Kusanovic, J. P.; Gorur, A.; Gotsch, F.; Webster, P.; Nhan-Chang, C.-L.; Erez, O.; Kim, C. J.; Espinoza, J.; Gonçalves, L. F.; Vaisbuch, E.; Mazaki-Tovi, S.; Hassan, S. S.; Costerton, J. W. Detection of a microbial biofilm in intraamniotic infection. *Am. J. Obstet. Gynecol.* **2008**, *198*, 135.e1−135.e5.
(7) Katsikogianni, M.; Missirlis, Y. F. Concise review of mechanisms of bacterial adhesion to biomaterials and of techniques used in estimating bacteria-material interactions. *Eur. Cells Mater.* **2004**, *8*, 37−57.
(8) Costerton, J. W.; Stewart, P. S.; Greenberg, E. P. Bacterial Biofilms: A Common Cause of Persistent Infections. *Science* **1999**, *284*, 1318−1322.

DOI: 10.1021/acsami.7b14416
ACS Appl. Mater. Interfaces 2017, 9, 44900−44910

(9) Singh, R.; Paul, D.; Jain, R. K. Biofilms: implications in bioremediation. *Trends Microbiol.* **2006**, *14*, 389−397.
(10) Trautner, B. W.; Lopez, A. I.; Kumar, A.; Siddiq, D. M.; Liao, K. S.; Li, Y.; Tweardy, D. J.; Cai, C. Nanoscale surface modification favors benign biofilm formation and impedes adherence by pathogens. *Nanomed. Nanotech. Biol. Med.* **2012**, *8*, 261−270.
(11) O'Toole, G.; Kaplan, H. B.; Kolter, R. Biofilm formation as microbial development. *Annu. Rev. Microbiol.* **2000**, *54*, 49−79.
(12) Dobosz, K. M.; Kolewe, K. W.; Schiffman, J. D. Green materials science and engineering reduces biofouling: approaches for medical and membrane-based technologies. *Front. Microbiol.* **2015**, *6*, 196.
(13) Gottenbos, B.; Busscher, H. J.; van der Mei, H. C.; Nieuwenhuis, P. Pathogenesis and prevention of biomaterial centered infections. *J. Mater. Sci.: Mater. Med.* **2002**, *13*, 717−722.
(14) Banerjee, I.; Pangule, R. C.; Kane, R. S. Antifouling Coatings: Recent Developments in the Design of Surfaces That Prevent Fouling by Proteins, Bacteria, and Marine Organisms. *Adv. Mater.* **2011**, *23*, 690−718.
(15) Roosjen, A.; van der Mei, H. C.; Busscher, H. J.; Norde, W. Microbial Adhesion to Poly(ethylene oxide) Brushes: Influence of Polymer Chain Length and Temperature. *Langmuir* **2004**, *20*, 10949−10955.
(16) Inoue, Y.; Nakanishi, T.; Ishihara, K. Elastic Repulsion from Polymer Brush Layers Exhibiting High Protein Repellency. *Langmuir* **2013**, *29*, 10752−10758.
(17) Holmlin, R. E.; Chen, X.; Chapman, R. G.; Takayama, S.; Whitesides, G. M. Zwitterionic SAMs that Resist Nonspecific Adsorption of Protein from Aqueous Buffer. *Langmuir* **2001**, *17*, 2841−2850.
(18) Kingshott, P.; Wei, J.; Bagge-Ravn, D.; Gadegaard, N.; Gram, L. Covalent Attachment of Poly(ethylene glycol) to Surfaces, Critical for Reducing Bacterial Adhesion. *Langmuir* **2003**, *19*, 6912−6921.
(19) Cheng, G.; Zhang, Z.; Chen, S.; Bryers, J. D.; Jiang, S. Inhibition of bacterial adhesion and biofilm formation on zwitterionic surfaces. *Biomaterials* **2007**, *28*, 4192−4199.
(20) Harbers, G. M.; Emoto, K.; Greef, C.; Metzger, S. W.; Woodward, H. N.; Mascali, J. J.; Grainger, D. W.; Lochhead, M. J. A functionalized poly(ethylene glycol)-based bioassay surface chemistry that facilitates bio-immobilization and inhibits non-specific protein, bacterial, and mammalian cell adhesion. *Chem. Mater.* **2007**, *19*, 4405−4414.
(21) Gon, S.; Kumar, K.-N.; Nüsslein, K.; Santore, M. M. How Bacteria Adhere to Brushy PEG Surfaces: Clinging to Flaws and Compressing the Brush. *Macromolecules* **2012**, *45*, 8373−8381.
(22) Yandi, W.; Mieszkin, S.; Martin-Tanchereau, P.; Callow, M. E.; Callow, J. A.; Tyson, L.; Liedberg, B.; Ederth, T. Hydration and Chain Entanglement Determines the Optimum Thickness of Poly(HEMA-*co*-PEG$_{10}$MA) Brushes for Effective Resistance to Settlement and Adhesion of Marine Fouling Organisms. *ACS Appl. Mater. Interfaces* **2014**, *6*, 11448−11458.
(23) Norde, W.; Gage, D. Interaction of Bovine Serum Albumin and Human Blood Plasma with PEO-Tethered Surfaces: Influence of PEO Chain Length, Grafting Density, and Temperature. *Langmuir* **2004**, *20*, 4162−4167.
(24) Inoue, Y.; Ishihara, K. Reduction of protein adsorption on well-characterized polymer brush layers with varying chemical structures. *Colloids Surf., B* **2010**, *81*, 350−357.
(25) Kobayashi, M.; Terayama, Y.; Yamaguchi, H.; Terada, M.; Murakami, D.; Ishihara, K.; Takahara, A. Wettability and Antifouling Behavior on the Surfaces of Superhydrophilic Polymer Brushes. *Langmuir* **2012**, *28*, 7212−7222.
(26) Terada, A.; Yuasa, A.; Kushimoto, T.; Tsuneda, S.; Katakai, A.; Tamada, M. Bacterial adhesion to and viability on positively charged polymer surfaces. *Microbiology* **2006**, *152*, 3575−3583.
(27) Mi, L.; Bernards, M. T.; Cheng, G.; Yu, Q.; Jiang, S. pH responsive properties of non-fouling mixed-charge polymer brushes based on quaternary amine and carboxylic acid monomers. *Biomaterials* **2010**, *31*, 2919−2925.
(28) Milner, S. T.; Witten, T. A.; Cates, M. E. Effects of polydispersity in the end-grafted polymer brush. *Macromolecules* **1989**, *22*, 853−861.
(29) de Vos, W. M.; Leermakers, F. A. M.; de Keizer, A.; Kleijn, J. M.; Cohen Stuart, M. A. Interaction of Particles with a Polydisperse Brush: A Self-Consistent-Field Analysis. *Macromolecules* **2009**, *42*, 5881−5891.
(30) Martin, T. B.; Dodd, P. M.; Jayaraman, A. Polydispersity for Tuning the Potential of Mean Force between Polymer Grafted Nanoparticles in a Polymer Matrix. *Phys. Rev. Lett.* **2013**, *110*, 018301.
(31) Bentz, K. C.; Savin, D. A. Chain Dispersity Effects on Brush Properties of Surface-Grafted Polycaprolactone-Modified Silica Nanoparticles: Unique Scaling Behavior in the Concentrated Polymer Brush Regime. *Macromolecules* **2017**, *50*, 5565−5573.
(32) Brault, N. D.; Sundaram, H. S.; Li, Y.; Huang, C.-J.; Yu, Q.; Jiang, S. Dry Film Refractive Index as an Important Parameter for Ultra-Low Fouling Surface Coatings. *Biomacromolecules* **2012**, *13*, 589−593.
(33) de Vos, W. M.; Leermakers, F. A. M. Modeling the structure of a polydisperse polymer brush. *Polymer* **2009**, *50*, 305−316.
(34) Qi, S.; Klushin, L. I.; Skvortsov, A. M.; Schmid, F. Polydisperse Polymer Brushes: Internal Structure, Critical Behavior, and Interaction with Flow. *Macromolecules* **2016**, *49*, 9665−9683.
(35) Ralston, E.; Swain, G. Bioinspiration—the solution for biofouling control? *Bioinspiration Biomimetics* **2009**, *4*, 015007.
(36) Cunliffe, D.; de las Heras Alarcón, C.; Peters, V.; Smith, J. R.; Alexander, C. Thermoresponsive Surface-Grafted Poly(N-isopropylacrylamide) Copolymers: Effect of Phase Transitions on Protein and Bacterial Attachment. *Langmuir* **2003**, *19*, 2888−2899.
(37) de las Heras Alarcón, C.; Farhan, T.; Osborne, V. L.; Huck, W. T. S.; Alexander, C. Bioadhesion at micro-patterned stimuli-responsive polymer brushes. *J. Mater. Chem.* **2005**, *15*, 2089−2094.
(38) Ista, L. K.; Mendez, S.; Lopez, G. P. Attachment and detachment of bacteria on surfaces with tunable and switchable wettability. *Biofouling* **2010**, *26*, 111−118.
(39) Wei, T.; Yu, Q.; Zhan, W.; Chen, H. A Smart Antibacterial Surface for the On-Demand Killing and Releasing of Bacteria. *Adv. Healthcare Mater.* **2016**, *5*, 449−456.
(40) Yan, S.; Shi, H.; Song, L.; Wang, X.; Liu, L.; Luan, S.; Yang, Y.; Yin, J. Nonleaching Bacteria-Responsive Antibacterial Surface Based on a Unique Hierarchical Architecture. *ACS Appl. Mater. Interfaces* **2016**, *8*, 24471−24481.
(41) Huang, C.-J.; Chen, Y.-S.; Chang, Y. Counterion-Activated Nanoactuator: Reversibly Switchable Killing/Releasing Bacteria on Polycation Brushes. *ACS Appl. Mater. Interfaces* **2015**, *7*, 2415−2423.
(42) Shivapooja, P.; Wang, Q.; Orihuela, B.; Rittschof, D.; López, G. P.; Zhao, X. Bioinspired Surfaces with Dynamic Topography for Active Control of Biofouling. *Adv. Mater.* **2013**, *25*, 1430−1434.
(43) Nakanishi, J.; Kikuchi, Y.; Takarada, T.; Nakayama, H.; Yamaguchi, K.; Maeda, M. Photoactivation of a Substrate for Cell Adhesion under Standard Fluorescence Microscopes. *J. Am. Chem. Soc.* **2004**, *126*, 16314−16315.
(44) Auernheimer, J.; Dahmen, C.; Hersel, U.; Bausch, A.; Kessler, H. Photoswitched Cell Adhesion on Surfaces with RGD Peptides. *J. Am. Chem. Soc.* **2005**, *127*, 16107−16110.
(45) Zhulina, E. B.; Birshtein, T. M.; Borisov, O. V. Theory of Ionizable Polymer Brushes. *Macromolecules* **1995**, *28*, 1491−1499.
(46) Yadav, V.; Harkin, A. V.; Robertson, M. L.; Conrad, J. C. Hysteretic memory in pH-response of water contact angle on poly(acrylic acid) brushes. *Soft Matter* **2016**, *12*, 3589−3599.
(47) Rosenberg, M.; Gutnick, D.; Rosenberg, E. Adherence of Bacteria to Hydrocarbons: A Simple Method for Measuring Cell-Surface Hydrophobicity. *FEMS Microbiol. Lett.* **1980**, *9*, 29−33.
(48) Wu, S. Surface and Interfacial Tensions of Polymer Melts. II. Poly(methyl methacrylate), Poly(n-butyl metharylate), and Polystyrene. *J. Phys. Chem.* **1970**, *74*, 632−638.
(49) Treat, N. D.; Ayres, N.; Boyes, S. G.; Brittain, W. J. A Facile Route to Poly(acrylic acid) Brushes Using Atom Transfer Radical Polymerization. *Macromolecules* **2006**, *39*, 26−29.

DOI: 10.1021/acsami.7b14416
ACS Appl. Mater. Interfaces 2017, 9, 44900−44910

(50) Wu, T.; Gong, P.; Szleifer, I.; Vlček, P.; Šubr, V.; Genzer, J. Behavior of Surface-Anchored Poly(acrylic acid) Brushes with Grafting Density Gradients on Solid Substrates: 1. Experiment. *Macromolecules* **2007**, *40*, 8756−8764.
(51) Schüwer, N.; Klok, H.-A. Tuning the pH Sensitivity of Poly(methacrylic acid) Brushes. *Langmuir* **2011**, *27*, 4789−4796.
(52) Cheesman, B. T.; Smith, E. G.; Murdoch, T. J.; Guibert, C.; Webber, G. B.; Edmondson, S.; Wanless, E. J. Polyelectrolyte brush pH-response at the silica−aqueous solution interface: a kinetic and equilibrium investigation. *Phys. Chem. Chem. Phys.* **2013**, *15*, 14502−14510.
(53) Sarkar, D.; Somasundaran, P. Conformational Dynamics of Poly(acrylic acid). A Study Using Surface Plasmon Resonance Spectroscopy. *Langmuir* **2004**, *20*, 4657−4664.
(54) Dong, R.; Lindau, M.; Ober, C. K. Dissociation Behavior of Weak Polyelectrolyte Brushes on a Planar Surface. *Langmuir* **2009**, *25*, 4774−4779.
(55) Aulich, D.; Hoy, O.; Luzinov, I.; Brücher, M.; Hergenröder, R.; Bittrich, E.; Eichhorn, K.-J.; Uhlmann, P.; Stamm, M.; Esser, N.; Hinrichs, K. In Situ Studies on the Switching Behavior of Ultrathin Poly(acrylic acid) Polyelectrolyte Brushes in Different Aqueous Environments. *Langmuir* **2010**, *26*, 12926−12932.
(56) Lu, Y.; Zhuk, A.; Xu, L.; Liang, X.; Kharlampieva, E.; Sukhishvili, S. A. Tunable pH and temperature response of weak polyelectrolyte brushes: role of hydrogen bonding and monomer hydrophobicity. *Soft Matter* **2013**, *9*, 5464−5472.
(57) Ruzicka, F.; Horka, M.; Hola, V.; Votava, M. Capillary Isoelectric Focusing—Useful tool for detection of the biofilm formation in Staphylococcus epidermidis. *J. Microbiol. Meth.* **2007**, *68*, 530−535.
(58) Jones, D. S.; Adair, C. G.; Mawhinney, W. M.; Gorman, S. P. Standardisation and comparison of methods employed for microbial cell surface hydrophobicity and charge determination. *Int. J. Pharm.* **1996**, *131*, 83−89.
(59) Sudagidan, M.; Erdem, I.; Cavusoglu, C.; Ciftçloğlu, M. Investigation of the surface properties of Staphylococcus epidermidis strains isolated from biomaterials. *Mikrobiyol. Bul.* **2010**, *44*, 93−103.
(60) Wu, T.; Gong, P.; Szleifer, I.; Vlček, P.; Šubr, V.; Genzer, J. Behavior of surface-anchored poly(acrylic acid) brushes with grafting density gradients on solid substrates: 1. Experiment. *Macromolecules* **2007**, *40*, 8756−8764.
(61) Ibanescu, S.-A.; Nowakowska, J.; Khanna, N.; Landmann, R.; Klok, H.-A. Effects of Grafting Density and Film Thickness on the Adhesion of Staphylococcus epidermidis to Poly(2-hydroxy ethyl methacrylate) and Poly(poly(ethylene glycol)methacrylate) Brushes. *Macromol. Biosci.* **2016**, *16*, 676−685.
(62) Chen, H.; Zhao, C.; Zhang, M.; Chen, Q.; Ma, J.; Zheng, J. Molecular Understanding and Structural-Based Design of Polyacrylamides and Polyacrylates as Antifouling Materials. *Langmuir* **2016**, *32*, 3315−3330.
(63) Yang, W.; Xue, H.; Li, W.; Zhang, J.; Jiang, S. Pursuing "Zero" Protein Adsorption of Poly(carboxybetaine) from Undiluted Blood Serum and Plasma. *Langmuir* **2009**, *25*, 11911−11916.
(64) Zhao, C.; Li, L.; Wang, Q.; Yu, Q.; Zheng, J. Effect of Film Thickness on the Antifouling Performance of Poly(hydroxy-functional methacrylates) Grafted Surfaces. *Langmuir* **2011**, *27*, 4906−4913.
(65) Chen, H.; Zhang, M.; Yang, J.; Zhao, C.; Hu, R.; Chen, Q.; Chang, Y.; Zheng, J. Synthesis and Characterization of Antifouling Poly(N-acryloylaminoethoxyethanol) with Ultralow Protein Adsorption and Cell Attachment. *Langmuir* **2014**, *30*, 10398−10409.
(66) Yang, W.; Chen, S.; Cheng, G.; Vaisocherová, H.; Xue, H.; Li, W.; Zhang, J.; Jiang, S. Film Thickness Dependence of Protein Adsorption from Blood Serum and Plasma onto Poly(sulfobetaine)-Grafted Surfaces. *Langmuir* **2008**, *24*, 9211−9214.
(67) Liu, Q.; Singh, A.; Liu, L. Amino Acid-Based Zwitterionic Poly(serine methacrylate) as an Antifouling Material. *Biomacromolecules* **2013**, *14*, 226−231.
(68) Halperin, A. Polymer Brushes that Resist Adsorption of Model Proteins: Design Parameters. *Langmuir* **1999**, *15*, 2525−2533.
(69) Jeon, S. I.; Lee, J. H.; Andrade, J. D.; De Gennes, P. G. Protein−surface interactions in the presence of polyethylene oxide. *J. Colloid Interface Sci.* **1991**, *142*, 149−158.
(70) de Vos, W. M.; Leermakers, F. A. M.; de Keizer, A.; Kleijn, J. M.; Cohen Stuart, M. A. Interaction of Particles with a Polydisperse Brush: A Self-Consistent Field Analysis. *Macromolecules* **2009**, *42*, 5881−5891.
(71) Wu, T.; Efimenko, K.; Genzer, J. Combinatorial Study of the Mushroom-to-Brush Crossover in Surface Anchored Polyacrylamide. *J. Am. Chem. Soc.* **2002**, *124*, 9394−9395.
(72) Mei, Y.; Wu, T.; Xu, C.; Langenbach, K. J.; Elliott, J. T.; Vogt, B. D.; Beers, K. L.; Amis, E. J.; Washburn, N. R. Tuning Cell Adhesion on Gradient Poly(2-hydroxyethyl methacrylate)-Grafted Surfaces. *Langmuir* **2005**, *21*, 12309−12314.
(73) Singh, N.; Cui, X.; Boland, T.; Husson, S. M. The role of independently variable grafting density and layer thickness of polymer nanolayers on peptide adsorption and cell adhesion. *Biomaterials* **2007**, *28*, 763−771.
(74) Wagner, V. E.; Koberstein, J. T.; Bryers, J. D. Protein and bacterial fouling characteristics of peptide and antibody decorated surfaces of PEG-poly(acrylic acid) co-polymers. *Biomaterials* **2004**, *25*, 2247−2263.

DOI: 10.1021/acsami.7b14416
ACS Appl. Mater. Interfaces 2017, 9, 44900−44910